RSC Advances

ROYAL SOCIETY OF CHEMISTRY

www.rsc.org/advances

Anions-Mediated Synthesis of Monodisperse Silver Nanoparticles and Useful for Screen Printing of High-Conductivity Patterns on Flexible Substrates for Printed Electronics

*L. Liu, X. X. Wan, L. L. Sun, S. L. Yang, Z. G. Dai, Q. Y. Tian, M. Lei , C. Z. Jiang and W. Wu**

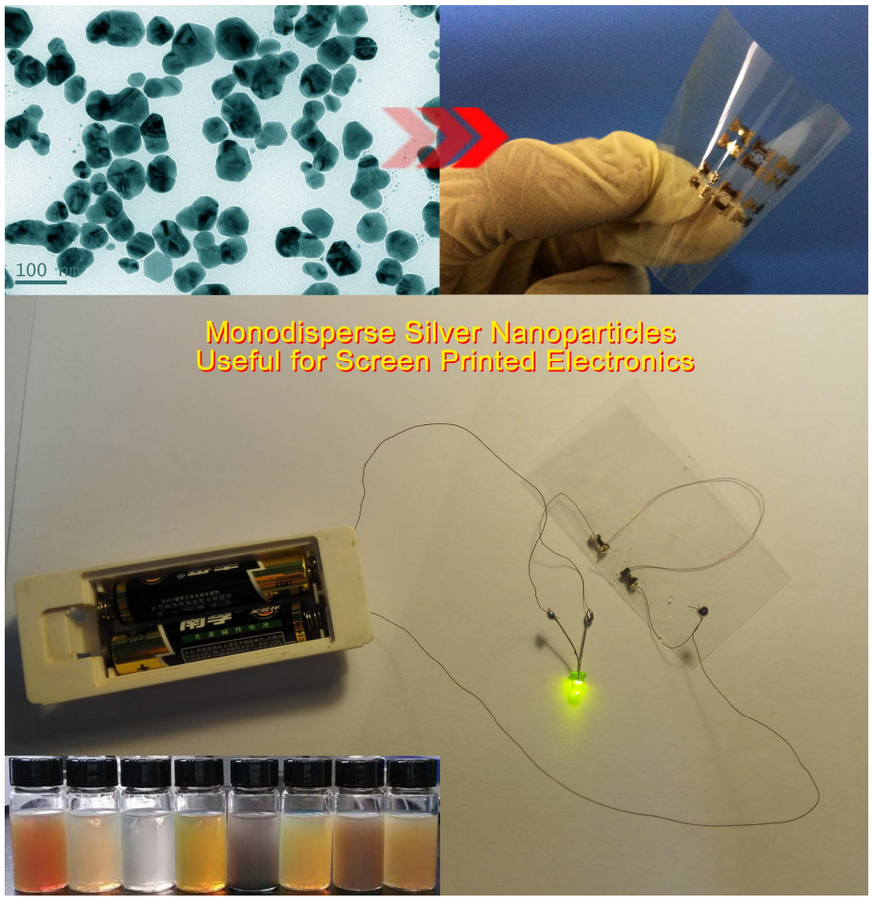

Anions-Mediated Synthesis of Monodisperse Silver Nanoparticles and Useful for Screen Printing of High-Conductivity Patterns on Flexible Substrates for Printed Electronics

*Li Liu[1], Xiaoxia Wan[1], Lingling Sun[1,3], Shuanglei Yang[1], Zhigao Dai[1,3], Qingyong Tian[1,3], Mei Lei[1,3], Xiangheng Xiao[3], Changzhong Jiang[3, 4] and Wei Wu[1,2,4]**

[1] Laboratory of Printable Functional Nanomaterials and Printed Electronics, School of Printing and Packaging, Wuhan University, Wuhan 430072, P. R. China

[2] Department of Physics and Materials Science and Center of Super Diamond and Advanced Films (COSDAF), City University of Hong Kong, Kowloon Tong, Hong Kong SAR

[3] Laboratory of Artificial Micro- and Nano-structures of Ministry of Education, School of Physics and Technology, Wuhan University, Wuhan 430072, P. R. China

[4] Shenzhen Research Institute of Wuhan University, Shenzhen 518057, P. R. China

Corresponding authors: weiwu@whu.edu.cn (W. Wu)

Abstract

Monodisperse silver nanoparticles (NPs) have been synthesized on a large scale by oxidation-reduction reaction in water via adding triethylamine to the aqueous solutions of $AgNO_3$, glucose and poly(vinyl pyrrolidone). Different anions, including $-SO_4^{2-}$, $-PO_4^{3-}$, $-CO_3^{2-}$ and $-Br^-$ are introduced to the above mixture to form slightly soluble silver compounds, which are used as the precursor to synthesize of silver NPs, the effect of silver nitrate/glucose ratio and reaction temperature are investigated. The electrical performance of the as-obtained Ag NPs have been studied, and the results reveal that the $-CO_3^{2-}$ mediate-synthesized Ag NPs process the lowest resistivity. The silver NPs can be well-dispersed in ethanol and generated as inks, which can be screen printed onto flexible polyester (PET) and paper substrates and formed conductive patterns after low-temperature sintering treatment. An optimal electrical resistivity can be reached to 5.72 μΩ·cm, which is much closed to the value of bulk silver (1.6 μΩ·cm). Obviously, the synthesized silver NPs could be considered as a cheap and effective material to have a great potential application for flexible printed electronics.

Keywords: silver NPs; anions-mediated synthesis; screen printing; flexible conductors.

1. Introduction:

Recently, there are a shift to develop simple approaches and techniques for fabricating electronic devices, and printing technologies have become a research focus and represent an emerging field. Owing to the ability to bypass traditional expensive and inflexible silicon-based electronics, printed electronics techniques could fabricate a variety of devices on flexible substrates, which is also being explored for the manufacture of large-area electronic devices by the patterned application of functional inks using high-throughput printing approaches.[1, 2] However, the critical issue that needs to be noticed when applying printed electronics to these applications is the development of high-performance and low-cost conductive inks. The development and integration of innovative printable electronic materials is a core activity since a diverse suite of materials is required for printed circuits, including high conductivity metals for electrodes and interconnects, high capacitance/low leakage gate dielectrics for capacitors and thin film transistors (TFTs), and high-mobility n-type and p-type semiconductors for complementary, low-power logic.

For designing and fabricating an optimal conductive ink, the ink preparing process should be both simple and high-yielding. The ink should possess a well printability, low viscosity and good stability to make it can be stored at room temperature and compatible with different printing technologies. Moreover, the patterned features should be highly conductive at room temperature and achieve bulk conductivity upon annealing at mild temperatures.[3] Though enormous efforts has been made in producing of conductive inks with different methods, it is still a key goal in modern materials chemistry and printed electronics field, and has drawn substantial attention in recent years. To date, conductive polymer,[4-6] carbon,[7, 8] graphene and graphene oxide,[9-13] and metallic nanoparticle inks[14-18] have been demonstrated. Recent progresses have concentrated on the fabricating and using their conductive inks for integration on various flexible substrates, such as textile, plastic and paper. Compared with the graphene and graphene oxide, metallic NPs is still low-cost and can be large-scaled production to meet industrial application. Since the discovery that metallic NPs show a reduced melting temperature compared to the bulk material, many studies have been conducted to form stabilized nanoparticle dispersions that can be printing, the use of silver NPs in conductive inks and its direct imaging by inkjet printing technology has been known that for years.[19-24] For example, Perelaer and co-workers fabricated silver-based conductive patterns by inkjet printing, which exhibited an excellent conductivity values of 5 to 56% of bulk silver.[25] Layani and co-workers have synthesized a conductive inks based on silver NPs, and it can be used to fabricate the 3D conductive patterns by inkjet printing.[26] In fact, with respect to the inkjet printing, the screen printing is a more convenient technique for industrial application.

On the other hand, the search for new geometries is an important aspect for noble metal nanomaterials, understanding the correlation between the sintering temperature, electronic properties of printed patterns/devices and the morphology of nanostructures is a prerequisite for widespread applications of printing electronics. Indeed, various experiment parameters, such as anions, temperature, contents of precursor and reducing agent, reduction time, which could result in the synthesize metal NPs for conductive ink with different properties.[14, 27-31] The building of various Ag nanostructures has achieved great success due to the development of synthetic methods. It is known that precipitates with a fairly low solubility will generate when the addition of different anions to aqueous solution of Ag^+ ions, this different chemical equilibrium which finally affect the nucleary of Ag NPs will occur in the reduction reaction to lead to the change of the morphology of Ag NPs.[32-34] For example, Li and co-workers have synthesized monodisperse, quasi-spherical Ag NPs directly in water via adding the aqueous solution of a mixture of AgNO3, sodium citrate, and the I^- ions were used to tailor the growth of the Ag NPs into a quasi-spherical shape via its preferential adsorption on the {111} facets.[35] Moreover, the different shapes of silver particles can generate different electrical performance in conductive ink.[36] For example, Yang and co-workers have reported the effect of the Ag particles, rods and plates in the conductive inks on electrical performance of the inkjet printed tracks by comparing the microstructure of three tracks, the results reveal that conductive ink filled with a mixture of nanorods and nanoparticles was more favorable to form random three-dimensionally interconnected conduction network to exhibit intriguing electrical characteristics.[37]

Encouraged by these aforementioned results, herein the present work was planned to interrogate how the morphology of Ag NPs formed upon addition of different anions including $-SO_4^{2-}$, $-PO_4^{3-}$, $-CO_3^{2-}$ and $-Br^-$ ions are obtained and the corresponding electronic performance after printed. We report a simple, environmentally friendly and cost-effective process for the preparation of monodisperse silver NPs for flexible printed electronics application. Different morphology of silver nanoparticles were synthesized and the effect of introduced anions ($-SO_4^{2-}$, $-PO_4^{3-}$, $-CO_3^{2-}$ and $-Br^-$) in reaction process were system investigated. The results of the conductivity of Ag electrodes reveal that the introduced carbonate ions is best, among in the phosphate ions, bromine ions and sulfate ions. Then, the other synthesized parameters of anions have been optimized and the corresponding conductivity of Ag electrodes have been studied, the conductivities as a function of sintering temperature and time were considered to achieve high conductive tracks, we also used the FE-SEM techniques to analyze the sintering mechanism of as-prepared Ag conductive inks. Our conductive ink that can be well applied to screen printing, it could be printed directly onto flexible substrates, such as PET and cellulose paper.

2. Experimental Sections

2.1 Materials and chemicals. Silver nitrate ($AgNO_3$, 99%) were purchased from Aladdin Chemistry Co., Ltd. Glucose ($C_6H_{12}O_6$, AR), Poly (N-vinylpyrrolidone) (PVP, GR), triethylamine (TEA, $C_6H_{15}N$, AR), anhydrous alcohol (C_2H_6O, AR), sodium sulfate (Na_2SO_4, AR), sodium carbonate (Na_2CO_3, AR) sodium phosphate (Na_3PO_4, AR) and sodium bromide (NaBr, AR) were purchased from Sinopharm Chemical Reagent Co., Ltd. The thickness of used high-temperature-resistant PET substrate is 0.3 mm, and the maximum bearing temperature is 230 °C. All the materials were used as received and without further purification in the whole experimental process. The deionized water was used throughout the experiments.

2.2 Synthesis of silver NPs at different reaction parameters. In our synthesis process, the silver nitrite was used as metal source, different anions were employed to tailor the morphology of products. $AgNO_3$, glucose, PVP and a given number of anions were consecutively added to water with stirring at room temperature, and then heated to the reaction temperature. TEA is added dropwise at a rate of ~0.6 mL/min into the solution by a peristaltic pump, and the color of the reaction solutions changed quickly. The reaction was lasted for 20 min. Finally, the resulting dispersion was washed three times by ethanol via centrifuge at 10000 rpm for 10 min. All the as-synthesized Ag NPs were washed perfectly to remove all the impurities before formulating inks. The synthesized silver NPs were re-dispersed in ethanol. The influences of the important synthesis parameters on the final product evolution were investigated through controlled studies on the morphology of Ag NPs, and the detailed reaction conditions are summarized in **Table 1**.

2.3 Preparation of silver films on PET substrate by direct deposition. Silver conductive ink was fabricated by re-disperse the as-synthesized silver NPs into ethanol and adjusting its concentration to 30 wt%. The PET substrates were cleaned by acetone and ethanol. After cleaning, the PET substrates were dried at room temperature prior to use. The silver colloids were dropped on the PET substrates by using a metal mask to finalize the design pattern (this pattern also can be screen printed on PET), and dried at room temperature to remove the solvent. The samples were dried at different temperatures in the range of 80-200 °C in an oven for 30 min, and then dried at 160 °C for different time with the range of 10~180 min.

2.4 Screen printing the Ag inks on cellulose paper substrate. Using this silver-based conductive ink, conductive lines, arrays, and printed circuit boards were manufactured on a paper substrate through screen printing. Screen printing was conducted out with 400 mesh counts' screen to form conductive patterns with different line widths (0.3, 0.4 and 0.5 mm).

2.5 Characterization. Field emission scanning electron microscopy (FE-SEM) images were carried out by using a high resolution field emission SEM (FEI Nova-400). The transmission electron microscopy (TEM), high-resolution TEM (HRTEM) images and energy-dispersive X-ray spectroscopy (EDX) analysis were performed on a JEOL JEM-2100F. The absorption spectra were recorded via UV-vis spectroscopy by a Shimadzu UV-2550 spectrophotometer. Electrical resistances of the samples were measured with a digital multimeter (victor 8245). All measurements were performed at room temperature.

3 Results and discussion

3.1 The morphology and product evolution of as-prepared Ag NPs

Many literatures have reported the synthesis of Ag NPs.[38-42] Herein, we investigate the morphology of Ag products synthesized in the present of different anions, including SO_4^{2-}, PO_4^{3-}, CO_3^{2-}, and Br^- ions. As shown **Figure 1**, Ag NPs were synthesized by reduction of silver nitrate with glucose using PVP as capping agent at different experimental parameters. Due to the importance of anions for the reduction, here we optimize the concentrations of anions used, details are at Supporting Information. The addition of these anions to the aqueous solution of Ag^+ is known to generate new silver compounds with slightly soluble in water, which impact on Ag^+ ions to synthesize Ag NPs via glucose/TEA reduction. The mechanism of silver ion reduction by glucose has been described by various reports.[43] In addition, the experimental process is easy to scale up, it only cost us 20 min to acquire nearly 5.2 g of Ag NPs in a 500 mL reaction mixture with a yield of 96%.

Owing to the different reaction parameters would influence the size and uniformity of the products, the TEM was used to investigate the morphology and size of as-synthesized silver NPs. **Figure 2** shows the TEM images of the as-obtained Ag NPs use different anions of PO_4^{3-}, SO_4^{2-}, Br^- and CO_3^{2-} ions. As shown in **Figure 2a**, when the SO_4^{2-} ions were introduced into the reaction (sample S1), the most of Ag NPs are spherical in shape and are well dispersed. And the insert representative SAED pattern is agrees with face centered cubic (*fcc*) crystalline structure of Ag NPs. When the PO_4^{3-} ions were introduced into the reaction (**Figure 2b**, sample S2), the as-obtained Ag NPs are mainly present in polygonal shape, and some Ag NPs are dumbbell in shape. When the CO_3^{2-} ions were introduced into the reaction (**Figure 2d**, sample S3), the as-obtained Ag NPs are mainly present in polygonal shape, and most numbers of Ag NPs are hexagon in shape. When the Br^- ions were introduced into the reaction (**Figure 2e**, sample S3), the as-obtained Ag NPs are mainly present in dumbbell shape. As shown in **Figure 2c and Figure 2f**, the average diameter of S1, S2, S3 and S4 is found to be approximately 49.2 nm, 43.7 nm, 68.4 nm and 53.1 nm, respectively. This different morphology and size of products suggest that anions can affect the

nucleation and the growth process during the formation of silver NPs. The above results further illustrate the anions can be used to tailored the shape of Ag NPs.

We also used the HRTEM and EDX to study the structure and composition of as-prepared Ag products. **Figure 3a** shows the representative HRTEM image of as-obtained individual Ag nanoparticle (sample S3), which reveals that the Ag nanoparticle possesses a good crystallinity. Combine with the FFT patterns, the fringes space at the edge is 0.235 nm, which can be indexed to the (111) facet of the *fcc* Ag. **Figure 3b** shows the EDX spectrum of the single Ag nanoparticle, the results display only Ag elements can be found (C and Cu belong to carbon film covered copper grid), no peaks of other impurity can be observed, which reveal the purity of as-synthesized Ag NPs.

Owing to the subsequent electronic characterization results reveal that the electronic properties of sample S3 is best, the morphology influence of the reaction temperature and molar concentration of the reductant were also studied. When the reaction temperature is decreased to 30 °C (sample S5), as shown in **Figure 4a**, the Ag NPs presents the polygonal shape. When the reaction temperature is increased to 90 °C (**Figure 4b,** sample S6), the polygonal shape of Ag NPs is still remained, but some large Ag NPs can be observed. **Figure 4c** shows the size histogram of the diameter of as-obtained Ag products, the average diameter of S5 and S6 is 54.0 nm and 56.5 nm, respectively. Compared with the sample S3 (**Figure 3f**), the mean diameter is decreased, which demonstrate the size distribution will be decreased when the temperature increased. However, the influence of the molar concentration of the reductant is not obviously. As shown in **Figure 4d** and **Figure 4e**, when the reducing agent is increased from 0.0015 ($AgNO_3$/glucose ratio = 2:1, sample S3) to 0.03 ($AgNO_3$/glucose ratio = 1:1, sample S7) and 0.06 ($AgNO_3$/glucose ratio = 1:2, sample S8), the polygonal shape of Ag NPs is still remained, and the average diameter of S7 and S8 is closed to the S3. The above results illustrate the reaction temperature can be used to tailored the size of Ag NPs.

Noble metal NPs often has a strong absorption in the visible area, this is due to the surface plasmon resonance (SPR) effect of the metal NPs. The intensity and location of SPR absorption peak can be used to forecast the size and morphology of the synthetized silver nanoparticle.[44, 45] In general, the absorption peak of Ag^+ ions is around 310 nm,[46] and the absorption bands of Ag NPs are in the range 380-620 nm.[47] **Figure 5** shows the photographs and UV-vis absorption spectra of Ag NPs (samples S1-S8) obtained at different reaction parameters. **Figure 5a** shows the photographs and UV-vis absorption spectra of Ag NPs of samples S1-S4) synthesized in the presence of different anions, it is obvious that there are changes in the color of samples and there are no absorption peak at about 310 nm, their SPR absorption peaks remain shifted, being centered at the range of 410-450 nm for the NPs obtained, the

shape of SPR absorption peaks is inerratic and symmetrical, indicating the Ag^{+} ions had been completely reduced to Ag NPs, and the increasing trend of SPR absorption peaks of each samples are consistent with the result of TEM and particle size distribution, the largest average size is obtained in the presence of $-CO_3^{2-}$ (sample S3). As shown in **Figure 5b**, the absorption peak moved and the maximal absorption peak is at 60 °C (sample S3). When the $AgNO_3$/glucose ratio change from 2:1 to 1:2, the absorption peak shift to left and color of samples obviously vary, as shown in **Figure 5c**.

3.2 The electronic properties of Ag tracks

Figure 6a shows the representative photographs of deposited Ag patterns (six electrodes) on PET substrates, the line width is 2.5 mm. The electrodes appear metallic gold yellow (see the insert photo), and the substrate can be severely bended and rolled without visible signs of Ag paint chipped, indicating the flexibility and mechanical robustness of the as-deposited Ag patterns. This feature implies possible application of the product in flexible printed electronics. **Figure 6b** shows the top-view SEM image of the surface of the electrodes was compose of the Ag NPs (sample S3), which shows no aggregates and a homogeneous dispersion over the large area. The cross-view SEM image was used to determine the thickness of the as-deposited Ag electrodes (sample S3), as shown in **Figure 6c**, the average thickness is about 715 nm. Subsequently, the electronic properties of Ag electrodes were measured, and the results reveal that the resistivity of S3 (use the CO_3^{2-} mediated-synthesized Ag NPs) is lowest, and if use the SO_4^{2-} mediated-synthesized Ag NPs, the resistivity can be up to 15000 μΩ·cm. Moreover, the changing of resistance of S3 as a function of bending times have been investigated, and the results demonstrate the resistance is enlarged 2.5 times and 4 times after 100 times bending at 90 º and 180 º, respectively (**Figure S1** in Support Information). The above reveal that the durability of printed electrode is good. And hence, we select the sample S3 was used the further investigation.

The sintering treatment is an important factor that determines the electronic performance of the deposited patterns, which can facilitate the removal of solvents and induce coalescence between silver NPs.[48] **Figure 7a** shows the electrical resistivity of patterns after heating at different temperatures for 30 min. It can be found the electrical resistivity will decrease with the increasing of sintering temperature. When the sintering temperature is 120 °C, the electrical resistivity is 9.8 μΩ·cm. It is noteworthy that if the Ag NPs are uniform and independent of each other without heat-treatment. As shown in **Figure 7b**, adjacent Ag NPs is start to melt and fuse together, and the surface is still smooth. When the sintering temperature is elevate to 160 °C, a clear melting and fusing phenomenon of adjacent Ag NPs can be observed in **Figure 7c**. The small agglomerates connected with each other and formed large agglomerates, and its resistivity was decreased from 9.8 μΩ·cm to 8.6 μΩ·cm. As shown in **Figure 7d**, all the adjacent Ag NPs is completely interconnected with each other when the sintering temperature is

reach to 200 °C, it cause its resistivity continuous decreased to 5.7 μΩ·cm, which is very closed to the value of bulk silver (1.6 μΩ·cm). It is noteworthy that the Ag NPs-based electrodes displays a lower resistivity compared with the referred results because the electrodes were manufactured by relatively large Ag NPs and without using any surfactants.[49-51] Clearly, the electrical resistivity is functionally related to the microstructure of Ag NPs-based electrodes. In addition, the necks between the adjacent Ag NPs can be observed that are well formed after sintering, which allows a percolation path for the electricity.

Moreover, the sintering time is another important factor to the electronic performance of the deposited patterns, and the **Figure 8a** shows the electrical resistivity of patterns after sintering treatment at 160 °C for different time. Obviously, the electrical resistivity will decrease with the prolonging of sintering time. The morphology of electrode surface were investigated and the representative SEM images were shown in **Figure 8b-d**, the changing of microstructure is similar to the SEM images of Ag electrodes as a function of sintering temperature, many necks between the Ag NPs can be well formed after elevate the sintering time. Because of the increase of necks, the electrical resistivity value is decrease from 11.4 μΩ·cm (sintering time is 10 min) to 6.7 μΩ·cm (sintering time is 150 min), and the SEM images of sintering time is 30 min (**Figure 8b**), 60 min (**Figure 8c**) and 90 min (**Figure 8d**) show a clear microstructural changing of the Ag patterns. Clearly, the conductivities of our Ag inks (only loading of 30 % Ag NPs) can be up to 25% that of bulk Ag with line widths as narrow as 2.5 mm with a mild sintering temperature and short sintering time.

Furthermore, we used the paper as substrate and then screen printed the above Ag inks as various patterns on the paper. Like as the PET, the paper-based flexible electronics is also attracted broad interest due to its huge commercial value in the future.[52-54] **Figure 9a** shows the photographs of screen plate, and the insert is the magnified patterns. Then these patterns were printed and sintered at 160 °C for 30 min in an oven. **Figure 9b** shows the photographs of printed patterns, and the average resistivity is 8.7 μΩ·cm. The above results demonstrate as-prepared Ag inks possess a good printability. This futures can be readily applied to various flexible electronics, including RFID antenna, solar cells, displays, sensors and smart labels.

4 Conclusions

In conclusion, the monodisperse Ag NPs were directly synthesized on a large scale by oxidation-reduction reaction, the effect of different introduced anions ($-SO_4^{2-}$, $-PO_4^{3-}$, $-CO_3^{2-}$ and $-Br^-$) in reaction process were systemic investigated. The conductive patterns on flexible PET and paper substrate with excellent electrical properties using as-obtained Ag NPs as the conductive inks, and the results of the fabricated conductivity of Ag electrodes reveal that the introduced carbonate ions is best, among in the

phosphate ions, bromine ions and sulfate ions. The optimal electrical resistivity is 5.7 μΩ·cm, which is only 3.6 times larger than that of bulk silver. Improved electrical resistivity can be attributed to the changing of microstructure after sintering treatment. It illuminates a promising route of directly printing electronics pattern on flexible substrates that will be very useful in a wide variety of practical application.

Acknowledgment

This work was partially supported by the NSFC (51201115, 51471121, 51171132, 11375134), Hong Kong Scholars Program, Young Chenguang Project of Wuhan City (2013070104010011), China Postdoctoral Science Foundation (2014M550406), Hubei Provincial Natural Science Foundation (2014CFB261), Basic Research Plan Program of Shenzhen City (No. JCYJ20130401160028783), the Fundamental Research Funds for the Central Universities and Wuhan University.

References

1. Minemawari, H.; Yamada, T.; Matsui, H.; Tsutsumi, J.; Haas, S.; Chiba, R.; Kumai, R.; Hasegawa, T., Inkjet printing of single-crystal films. *Nature* **2011,** *475*, 364-367.

2. Wu, W.; Changzhong, J.; Roy, V. A. L., Recent progress in magnetic iron oxide-semiconductor composite nanomaterials as promising photocatalysts. *Nanoscale* **2015,** *7*, 38-58.

3. Walker, S. B.; Lewis, J. A., Reactive Silver Inks for Patterning High-Conductivity Features at Mild Temperatures. *J. Am. Chem. Soc.* **2012,** *134*, 1419-1421.

4. Kang, B.; Lee, W. H.; Cho, K., Recent Advances in Organic Transistor Printing Processes. *ACS Appl. Mater. Interfaces* **2013,** *5*, 2302-2315.

5. Kwak, D.; Lim, J. A.; Kang, B.; Lee, W. H.; Cho, K., Self‐Organization of Inkjet‐Printed Organic Semiconductor Films Prepared in Inkjet‐Etched Microwells. *Adv. Funct. Mater.* **2013**.

6. Park, K. S.; Cho, B.; Baek, J.; Hwang, J. K.; Lee, H.; Sung, M. M., Single‐Crystal Organic Nanowire Electronics by Direct Printing from Molecular Solutions. *Adv. Funct. Mater.* **2013**.

7. Huang, L.; Huang, Y.; Liang, J.; Wan, X.; Chen, Y., Graphene-based conducting inks for direct inkjet printing of flexible conductive patterns and their applications in electric circuits and chemical sensors. *Nano Res* **2011,** *4*, 675-684.

8. Han, X.; Chen, Y.; Zhu, H.; Preston, C.; Wan, J.; Fang, Z.; Hu, L., Scalable, printable, surfactant-free graphene ink directly from graphite. *Nanotechnology* **2013,** *24*, 205304.

9. Xie, Y.; Lohrman, J.; Ren, S., Phase aggregation and morphology effects on nanocarbon optoelectronics. *Nanotechnology* **2014,** *25*, 485601.

10. Nolan, H.; Mendoza-Sanchez, B.; Kumar, N. A.; McEvoy, N.; O'Brien, S.; Nicolosi, V.; Duesberg, G. S., Nitrogen-doped reduced graphene oxide electrodes for electrochemical supercapacitors. *Physical Chemistry Chemical Physics* **2014,** *16*, 2280-2284.

11. Bai, Y.-F.; Zhang, Y.-F.; Zhou, A.-W.; Li, H.-W.; Zhang, Y.; Luong, J. H.; Cui, H.-F., Self-assembly of a thin highly reduced graphene oxide film and its high electrocatalytic activity. *Nanotechnology* **2014,** *25*, 405601.

12. Islam, R.; Chan-Yu-King, R.; Brun, J.-F.; Gors, C.; Addad, A.; Depriester, M.; Hadj-Sahraoui, A.; Roussel, F., Transport and thermoelectric properties of polyaniline/reduced graphene oxide nanocomposites. *Nanotechnology* **2014,** *25*, 475705.

13. Kim, H. Y.; Jang, K. J.; Veerapandian, M.; Kim, H. C.; Seo, Y. T.; Lee, K. N.; Lee, M.-H., Reusable urine glucose sensor based on functionalized graphene oxide conjugated Au electrode with protective layers. *Biotechnology Reports* **2014,** *3*, 49-53.

14. Tang, X.-F.; Yang, Z.-G.; Wang, W.-J., A simple way of preparing high-concentration and high-purity nano copper colloid for conductive ink in inkjet printing technology. *"Colloids Surf. A "* **2010,** *360*, 99-104.

15. Jeong, S.; Song, H. C.; Lee, W. W.; Choi, Y.; Ryu, B.-H., Preparation of aqueous Ag Ink with long-term dispersion stability and its inkjet printing for fabricating conductive tracks on a polyimide film. *J. Appl. Phys.* **2010,** *108*, 102805-102805-5.

16. Jo, Y. H.; Jung, I.; Choi, C. S.; Kim, I.; Lee, H. M., Synthesis and characterization of low temperature Sn nanoparticles for the fabrication of highly conductive ink. *Nanotechnology* **2011,** *22*, 225701.

17. Shankar, R.; Groven, L.; Amert, A.; Whites, K. W.; Kellar, J. J., Non-aqueous synthesis of silver nanoparticles using tin acetate as a reducing agent for the conductive ink formulation in printed electronics. *J. Mater. Chem.* **2011,** *21*, 10871-10877.

18. Anto, B. T.; Sivaramakrishnan, S.; Chua, L. L.; Ho, P. K., Hydrophilic Sparse Ionic Monolayer - Protected Metal Nanoparticles: Highly Concentrated Nano- Au and Nano- Ag "Inks" that can be Sintered to Near- Bulk Conductivity at 150° C. *Adv. Funct. Mater.* **2010,** *20*, 296-303.

19. Kordás, K.; Mustonen, T.; Tóth, G.; Jantunen, H.; Lajunen, M.; Soldano, C.; Talapatra, S.; Kar, S.; Vajtai, R.; Ajayan, P. M., Inkjet printing of electrically conductive patterns of carbon nanotubes. *Small* **2006,** *2*, 1021-1025.

20. Vaillancourt, J.; Zhang, H.; Vasinajindakaw, P.; Xia, H.; Lu, X.; Han, X.; Janzen, D. C.; Shih, W.-S.; Jones, C. S.; Stroder, M., All ink-jet-printed carbon nanotube thin-film transistor on a polyimide

substrate with an ultrahigh operating frequency of over 5 GHz. *Applied Physics Letters* **2008,** *93*, 243301.

21. Yabuki, A.; Arriffin, N.; Yanase, M., Low-temperature synthesis of copper conductive film by thermal decomposition of copper–amine complexes. *Thin Solid Films* **2011,** *519*, 6530-6533.

22. Jeong, S.; Song, H. C.; Lee, W. W.; Lee, S. S.; Choi, Y.; Son, W.; Kim, E. D.; Paik, C. H.; Oh, S. H.; Ryu, B.-H., Stable aqueous based Cu nanoparticle ink for printing well-defined highly conductive features on a plastic substrate. *Langmuir* **2011,** *27*, 3144-3149.

23. Perelaer, J.; de Gans, B. J.; Schubert, U. S., Ink- jet Printing and Microwave Sintering of Conductive Silver Tracks. *Advanced materials* **2006,** *18*, 2101-2104.

24. Lee, H.-H.; Chou, K.-S.; Huang, K.-C., Inkjet printing of nanosized silver colloids. *Nanotechnology* **2005,** *16*, 2436.

25. Perelaer, J.; de Laat, A. W.; Hendriks, C. E.; Schubert, U. S., Inkjet-printed silver tracks: low temperature curing and thermal stability investigation. *Journal of Materials Chemistry* **2008,** *18*, 3209-3215.

26. Layani, M.; Cooperstein, I.; Magdassi, S., UV crosslinkable emulsions with silver nanoparticles for inkjet printing of conductive 3D structures. *Journal of Materials Chemistry C* **2013,** *1*, 3244-3249.

27. Jiang, X.; Yu, A., Silver nanoplates: a highly sensitive material toward inorganic anions. *Langmuir* **2008,** *24*, 4300-4309.

28. Zhai, D.; Zhang, T.; Guo, J.; Fang, X.; Wei, J., Water-based ultraviolet curable conductive inkjet ink containing silver nano-colloids for flexible electronics. *Colloids and Surfaces A: Physicochemical and Engineering Aspects* **2013,** *424*, 1-9.

29. Pacioni, N. L.; Pardoe, A.; McGilvray, K. L.; Chrétien, M. N.; Scaiano, J. C., Synthesis of copper nanoparticles mediated by photogenerated free radicals: catalytic role of chloride anions. *Photochemical & Photobiological Sciences* **2010,** *9*, 766-774.

30. Stamplecoskie, K. G.; Scaiano, J. C., Light emitting diode irradiation can control the morphology and optical properties of silver nanoparticles. *Journal of the American Chemical Society* **2010,** *132*, 1825-1827.

31. Maretti, L.; Billone, P. S.; Liu, Y.; Scaiano, J. C., Facile photochemical synthesis and characterization of highly fluorescent silver nanoparticles. *Journal of the American Chemical Society* **2009,** *131*, 13972-13980.

32. Li, H.; Xia, H.; Ding, W.; Li, Y.; Shi, Q.; Wang, D.; Tao, X., Synthesis of Monodisperse, Quasi-Spherical Silver Nanoparticles with Sizes Defined by the Nature of Silver Precursors. *Langmuir* **2014,** *30*, 2498-2504.

33. Masango, S. S.; Peng, L.; Marks, L. D.; Van Duyne, R. P.; Stair, P. C., Nucleation and Growth of Silver Nanoparticles by AB and ABC-Type Atomic Layer Deposition. *J. Phys. Chem. C* **2014,** *118*, 17655-17661.

34. Pacioni, N. L.; Pardoe, A.; McGilvray, K. L.; Chretien, M. N.; Scaiano, J. C., Synthesis of copper nanoparticles mediated by photogenerated free radicals: catalytic role of chloride anions. *Photochemical & Photobiological Sciences* **2010,** *9*, 766-774.

35. Li, H.; Xia, H.; Wang, D.; Tao, X., Simple Synthesis of Monodisperse, Quasi-spherical, Citrate-Stabilized Silver Nanocrystals in Water. *Langmuir* **2013,** *29*, 5074-5079.

36. Suriati, G.; Mariatti, M.; Azizan, A., Effects of filler shape and size on the properties of silver filled epoxy composite for electronic applications. *J Mater Sci: Mater Electron* **2011,** *22*, 56-63.

37. Yang, X.; He, W.; Wang, S.; Zhou, G.; Tang, Y.; Yang, J., Effect of the different shapes of silver particles in conductive ink on electrical performance and microstructure of the conductive tracks. *J Mater Sci: Mater Electron* **2012,** *23*, 1980-1986.

38. Ryu, B.-H.; Choi, Y.; Park, H.-S.; Byun, J.-H.; Kong, K.; Lee, J.-O.; Chang, H., Synthesis of highly concentrated silver nanosol and its application to inkjet printing. *Colloids and Surfaces A: Physicochemical and Engineering Aspects* **2005,** *270*, 345-351.

39. Lee, C.-L.; Chang, K.-C.; Syu, C.-M., Silver nanoplates as inkjet ink particles for metallization at a low baking temperature of 100 C. *Colloids and Surfaces A: Physicochemical and Engineering Aspects* **2011,** *381*, 85-91.

40. Banerjee, S.; Loza, K.; Meyer-Zaika, W.; Prymak, O.; Epple, M., Structural Evolution of Silver Nanoparticles during Wet-Chemical Synthesis. *Chemistry of Materials* **2014,** *26*, 951-957.

41. Lu, L.; Liu, J.; Hu, Y.; Zhang, Y.; Chen, W., Graphene‐Stabilized Silver Nanoparticle Electrochemical Electrode for Actuator Design. *Advanced Materials* **2013,** *25*, 1270-1274.

42. Kumar, S.; Selvaraj, C.; Scanlon, L.; Munichandraiah, N., Ag nanoparticles–anchored reduced graphene oxide catalyst for oxygen electrode reaction in aqueous electrolytes and also a non-aqueous electrolyte for Li–O 2 cells. *Physical Chemistry Chemical Physics* **2014,** *16*, 22830-22840.

43. Wang, H.; Qiao, X.; Chen, J.; Ding, S., Preparation of silver nanoparticles by chemical reduction method. *Colloids and Surfaces A: Physicochemical and Engineering Aspects* **2005,** *256*, 111-115.

44. Sherry, L. J.; Jin, R.; Mirkin, C. A.; Schatz, G. C.; Van Duyne, R. P., Localized surface plasmon resonance spectroscopy of single silver triangular nanoprisms. *Nano letters* **2006,** *6*, 2060-2065.

45. Wiley, B. J.; Im, S. H.; Li, Z.-Y.; McLellan, J.; Siekkinen, A.; Xia, Y., Maneuvering the surface plasmon resonance of silver nanostructures through shape-controlled synthesis. *The Journal of Physical Chemistry B* **2006,** *110*, 15666-15675.

46. Janata, E.; Henglein, A.; Ershov, B., First clusters of Ag+ ion reduction in aqueous solution. *The Journal of Physical Chemistry* **1994,** *98*, 10888-10890.

47. Christy, A. J.; Umadevi, M., Synthesis and characterization of monodispersed silver nanoparticles. *Advances in Natural Sciences: Nanoscience and Nanotechnology* **2012,** *3*, 035013.

48. Merilampi, S.; Laine-Ma, T.; Ruuskanen, P., The characterization of electrically conductive silver ink patterns on flexible substrates. *Microelectronics reliability* **2009,** *49*, 782-790.

49. Lee, Y.-I.; Kim, S.; Jung, S.-B.; Myung, N. V.; Choa, Y.-H., Enhanced Electrical and Mechanical Properties of Silver Nanoplatelet-Based Conductive Features Direct Printed on a Flexible Substrate. *ACS applied materials & interfaces* **2013,** *5*, 5908-5913.

50. Ahn, B. Y.; Duoss, E. B.; Motala, M. J.; Guo, X.; Park, S.-I.; Xiong, Y.; Yoon, J.; Nuzzo, R. G.; Rogers, J. A.; Lewis, J. A., Omnidirectional printing of flexible, stretchable, and spanning silver microelectrodes. *Science* **2009,** *323*, 1590-1593.

51. Zhang, Z.; Zhang, X.; Xin, Z.; Deng, M.; Wen, Y.; Song, Y., Synthesis of monodisperse silver nanoparticles for ink-jet printed flexible electronics. *Nanotechnology* **2011,** *22*, 425601.

52. Wong, W. S.; Salleo, A., *Flexible electronics: materials and applications*. Springer: 2009; Vol. 24.

53. Russo, A.; Ahn, B. Y.; Adams, J. J.; Duoss, E. B.; Bernhard, J. T.; Lewis, J. A., Pen‐on‐Paper Flexible Electronics. *Advanced materials* **2011,** *23*, 3426-3430.

54. Hu, A.; Guo, J.; Alarifi, H.; Patane, G.; Zhou, Y.; Compagnini, G.; Xu, C., Low temperature sintering of Ag nanoparticles for flexible electronics packaging. *Applied Physics Letters* **2010,** *97*, 153117.

Figure Captions

Figure 1. Schematic illustration of the synthesis process of Ag NPs in the presence of different anions.

Figure 2. TEM images of synthesized Ag NPs in the presence of different anions: (a) SO_4^{2-}, the insert is the representative SAED pattern, (b) PO_4^{3-}, (d) CO_3^{2-}, (e) Br^- and corresponding histogram of particle size distributions (c and f).

Figure 3. The HRTEM image of Ag NPs, the inset are fast Fourier transformation (FFT) pattern (a); EDX spectra of the single Ag NPs, the inset table is the composition of the silver particles (b, the peaks located at the binding energies of 0.28, 0.95, 8.05 and 8.92 keV belong to C and Cu signal of carbon film covered copper grid).

Figure 4. TEM images of synthesized silver NPs (synthesized in the presence of CO_3^{2-}) at different temperature: (a) 30 °C, (b) 90 °C and at different ratio of n($AgNO_3$)/n(Glucose): (d) 1:1 (e) 1:2. (c) and (f) are the corresponding histogram of particle size distributions.

Figure 5. Photographs of the as-obtained Ag NPs solution and the UV-vis absorption spectra at different reaction parameters:(a) in the presence of SO_4^{2-}, PO_4^{3-} , CO_3^{2-} and Br^-; (b) at different temperature: 30 °C, 60°C and 90 °C; (c) at different ratio of n($AgNO_3$)/n(Glucose): 2:1, 1:1 and 1:2.

Figure 6. Optical image of silver patterns deposited on PET substrate and dried at room temperature without sintering-treatment (a); Top-view (b) and cross-view SEM image (b) of the silver tracks formed after sintering at 160 °C for 30 min; Electrical resistivity of silver conductive patterns of all samples of S1-S8 (d).

Figure 7. Electrical resistivity of patterns after sintering at different temperatures for 30 min (a); Representative SEM images of silver patterns on PET substrates sintered in an oven at different temperature: 120 °C (b), 160 °C (c), and 200 °C (d).

Figure 8. Electrical resistivity of patterns after sintering at 160°C for different time (a); Representative SEM images of silver patterns on PET substrates sintered in an oven at different time: 30min (b), 60min (c), and 90min (d).

Figure 9. Photographs of screen printing plate (a) and the different conductive patterns on the paper by screen printing of the as-prepared silver NPs (b, sample S3).

Figures

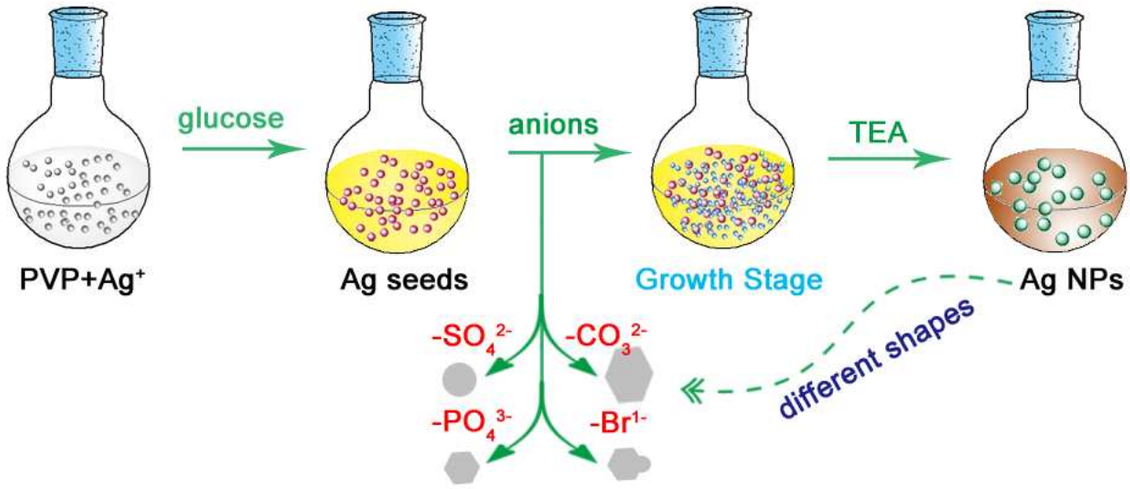

Figure 1

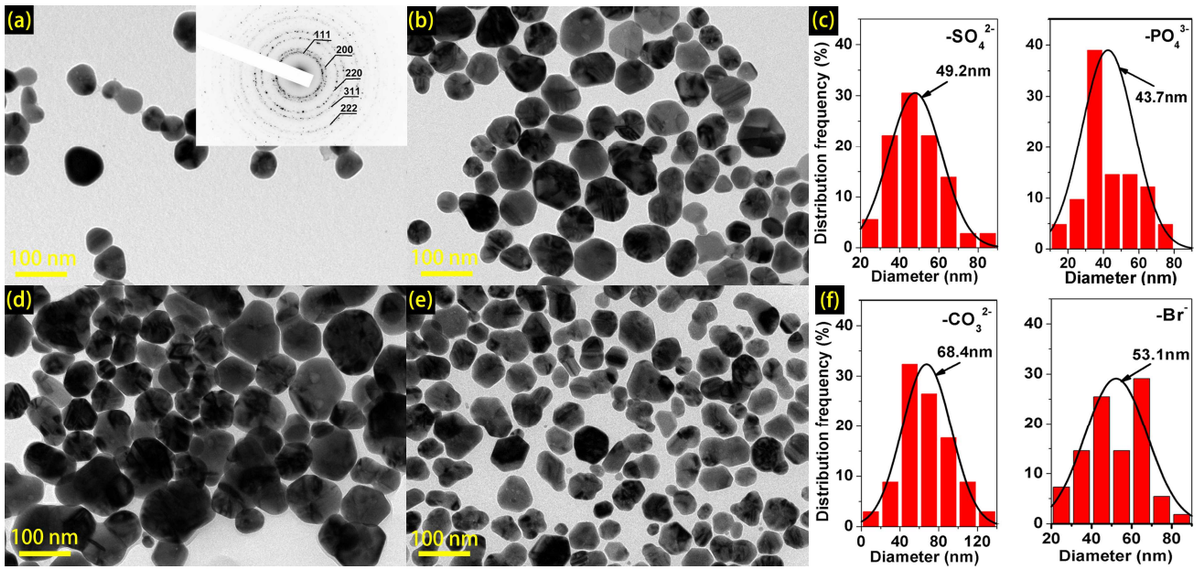

Figure 2

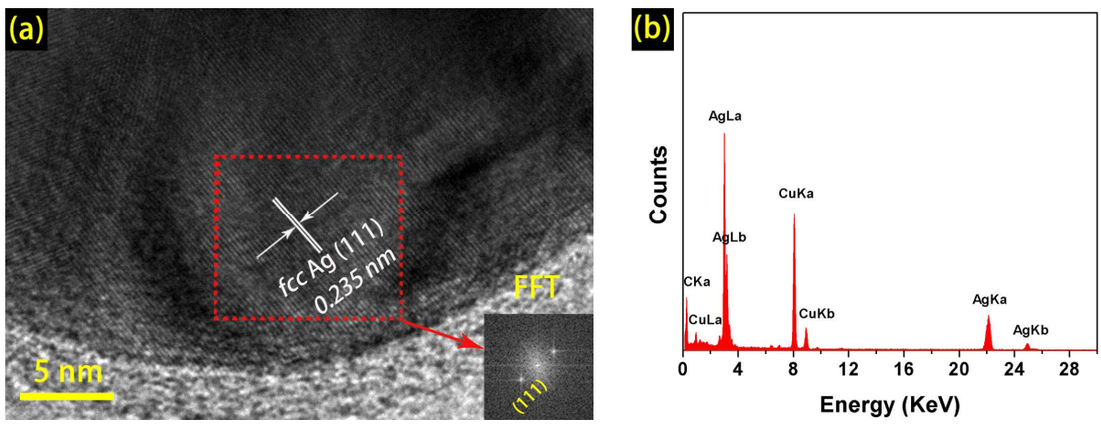

Figure 3

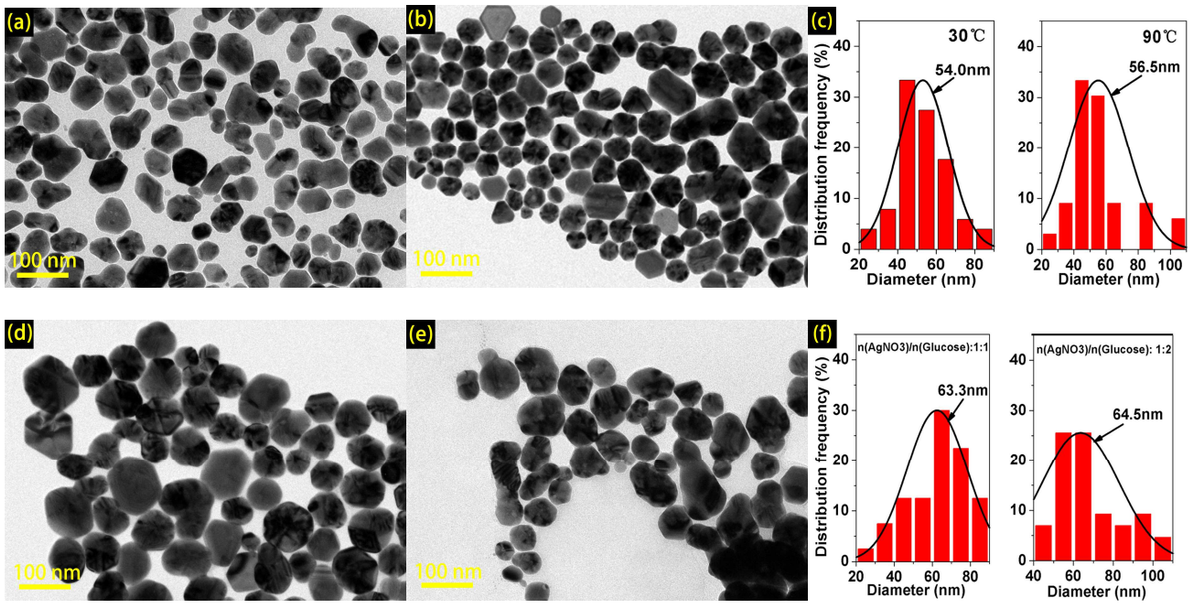

Figure 4

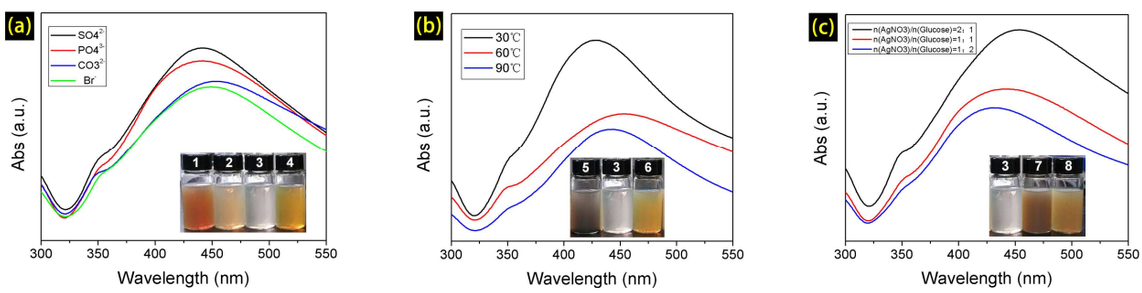

Figure 5

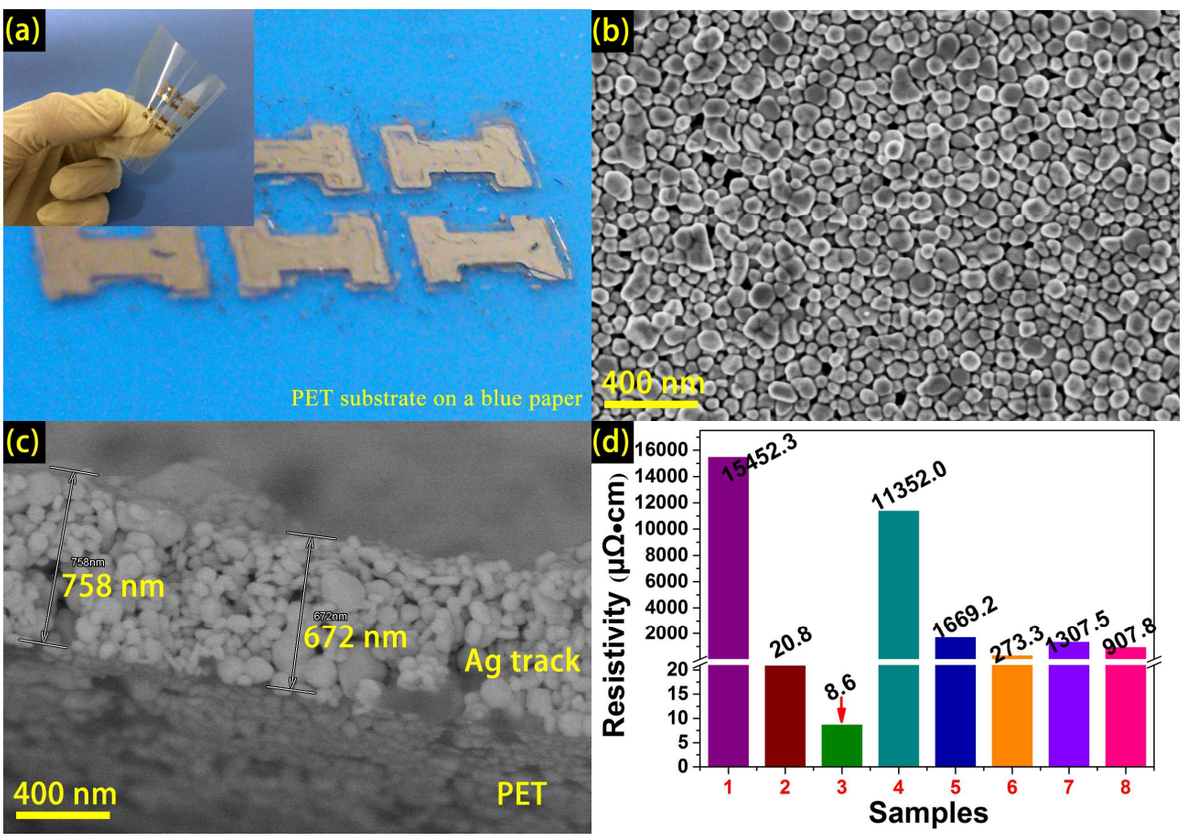

Figure 6

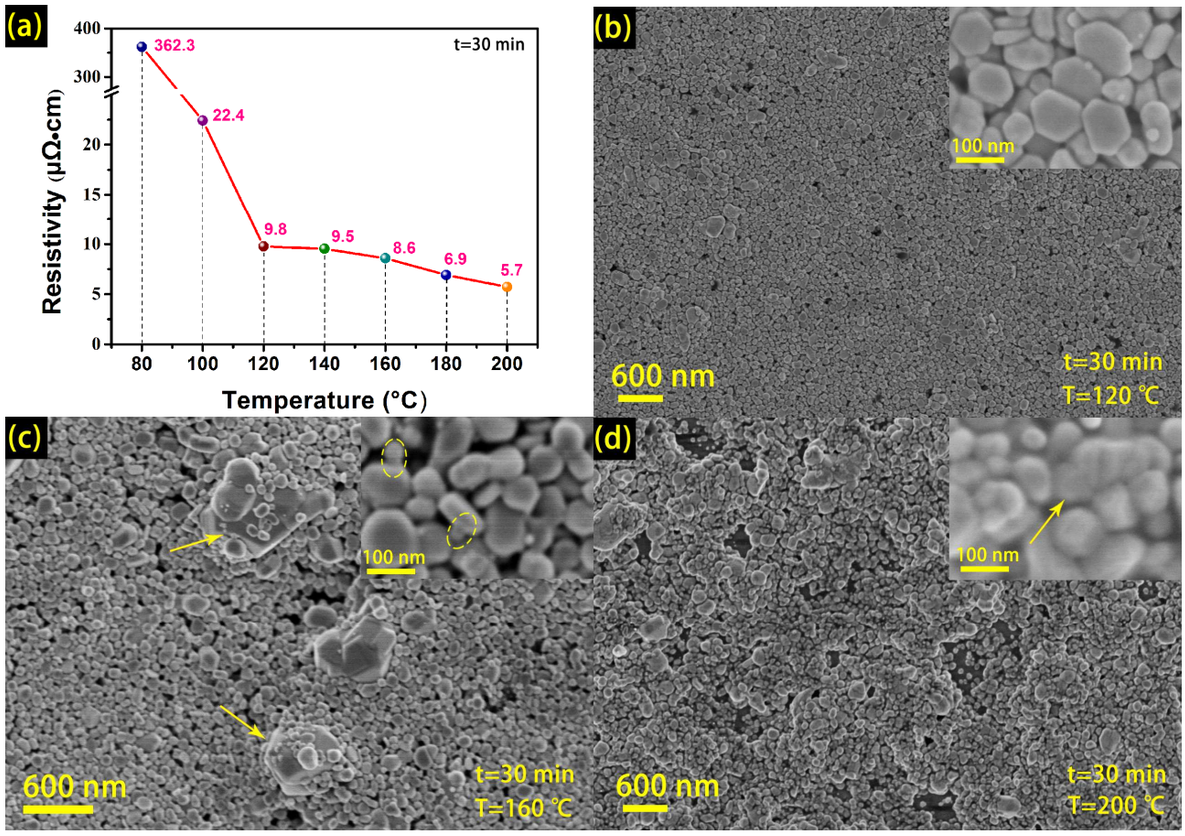

Figure 7

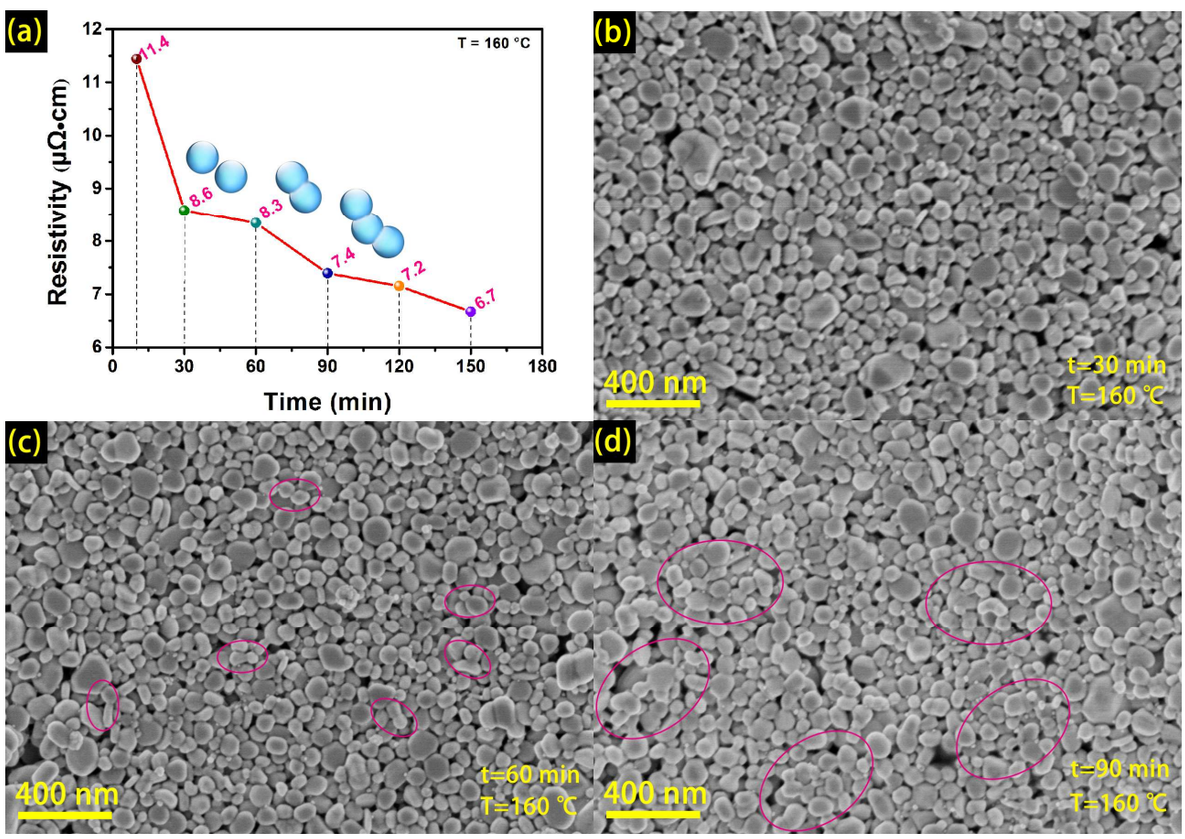

Figure 8

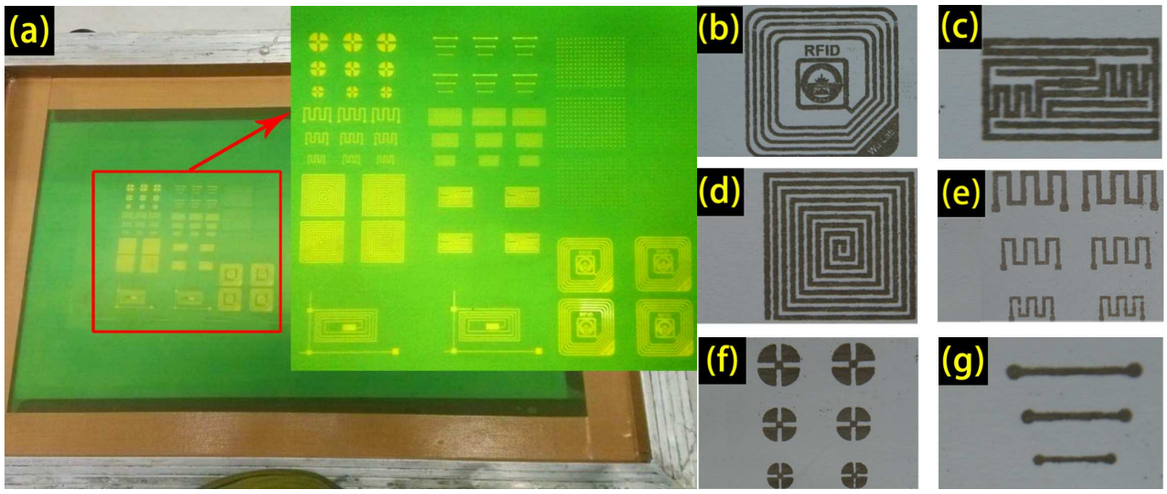

Figure 9

Table

Table 1 Synthesis conditions for the preparation of silver particles.

Sample ID	Reducing agent (M)	PVP (g)	Et_3N (μL)	Reaction temperature (°C)	Anion	Silver nitrate (mol)	Reaction time (min)
1	0.0015	1	300	60	SO_4^{2-}	0.003	20
2	0.0015	1	300	60	PO_4^{3-}	0.003	20
3	0.0015	1	300	60	CO_3^{2-}	0.003	20
4	0.0015	1	300	60	Br^-	0.003	20
5	0.0015	1	300	30	CO_3^{2-}	0.003	20
6	0.0015	1	300	90	CO_3^{2-}	0.003	20
7	0.003	1	300	60	CO_3^{2-}	0.003	20
8	0.006	1	300	60	CO_3^{2-}	0.003	20